Proceedings of the 14th International Scientific and Practical Conference «Global and Regional Aspects of Sustainable Development»

(September 16-18, 2026). Copenhagen, Denmark

No 309

RADIO ENGINEERING, ELECTRONICS AND ELECTRICAL ENGINEERING

Hardware-in-the-Loop Evaluation of an ESP32 BLE-to-LoRa Bridge for a Two-Axis Antenna Rotator

Kovalchuk Bohdan P. [1], Ivko Serhii O. [2]

[1]Candidate of Physical and Mathematical Sciences, Head of Research Laboratory;
Military Institute of Telecommunications and Information Technologies named after the Heroes of Kruty; Ukraine

[2]Candidate of Technical Sciences, Senior Research Fellow;
Military Institute of Telecommunications and Information Technologies named after the Heroes of Kruty; Ukraine

Abstract. Extending the control path of a two-axis antenna rotator beyond Bluetooth Low Energy (BLE) range must preserve command integrity and pointing accuracy. This study presents and hardware-in-the-loop evaluates an ESP32 bridge that retains direct BLE and adds point-to-point LoRa through RA-02 modules. The completed campaign covered 43 planned items across direct BLE, BLE-to-LoRa relay, and Internet access. The protocol combined functional acceptance checks with retained serial instrumentation and firmware-path inspection. Authenticated frames returned acknowledgments, encoder angles, link state, and radio-quality telemetry over the same half-duplex channel. Of 37 executed items, 34 fully passed (91.9%), one was partial, and two failed; six items requiring destructive, unavailable-rig, or human-only conditions were reported separately. Signed 5-degree jogs and coordinate pointing executed over both direct and relayed paths. Maximum observed settled two-axis error was approximately 1.3 degrees for direct BLE and 1.0 degree for the bridge, both within the 1.5-degree control tolerance. During a 30 s bridge hold, all 126 samples reported link up, with received signal strength from −79 to −77 dBm and signal-to-noise ratio from 9.2 to 12.0 dB. Both failures affected mutual peer sessions. Serial evidence and transmit-path analysis identified an immediate LoRa branch without clear-channel assessment; the corrective guard was integrated into firmware. The study confirms completed hardware integration, stable manual and coordinate control through the bridge, and a technically grounded correction to half-duplex scheduling.
Keywords: *antenna pointing; ESP32; Bluetooth Low Energy; LoRa; two-axis rotator; hardware-in-the-loop testing.*

Introduction. A mechanically pointed antenna is driven by two loops: the node closes the position loop, and an operator link sets the target. Command integrity on that link is a design constraint alongside mechanical accuracy: pointing designs derive the admissible error from link budgets [1], dual-mode designs exercise two modes on one tracker [2], and operational studies pair axis behavior with received-signal data [3]. This end-to-end view treats command delivery, mechanical response, and feedback visibility as one control transaction rather than as separate radio and motion tests.

LoRa gives long range from modest hardware, but its behavior follows from configuration. Packet reception depends on physical-layer settings and packet length [4], and nominal range does not establish reliability [5]. Delay and loss vary with payload, air data rate, power, and environment [6]. Acknowledgments make an outcome observable without removing contention [7], so latency-bound traffic needs an explicit schedule [8], and networked control measures latency at the application boundary, not at the radio [9]. Consequently, bridge evaluation must combine end-to-end command execution, returned state, recovery behavior, and scheduling under competing bidirectional traffic.

The bridge components are documented: RA-02 modules operating within the SX1276/77/78/79 device-family ranges [10], an ESP32 supplying SPI and BLE [11], and BLE access conforming to the Bluetooth Core Specification [12]. The LoRa Wide Area Network studies [7], [8] provide scheduling context rather than evidence for this point-to-point link, while the 802.11ax study [9] contributes application-boundary latency methodology. Within the reviewed literature, no study reports a system-level hardware-in-the-loop evaluation in which direct BLE and BLE-to-LoRa paths drive the same rotator across control, recovery, and cross-transport scenarios.

Objective. The objective is to design, integrate, and experimentally evaluate an ESP32 BLE-to-LoRa bridge for a two-axis antenna rotator, quantify functional test coverage and pointing accuracy on the assembled hardware, and determine the mechanism of any reproducible communication-path failures.

System architecture. The implemented signal path is shown in Fig. 1. An Android application sends JavaScript Object Notation (JSON) or plain-text commands over a Bluetooth Low Energy Generic Attribute Profile (BLE GATT) service to the bridge ESP32. The bridge maps accepted messages to Nanopb Protocol Buffers and forwards them through point-to-point LoRa. The remote ESP32 node drives two BTS7960 motor drivers and measures azimuth and elevation with two AS5600 absolute magnetic encoders; telemetry and acknowledgments return through the same half-duplex path. A precise jog adds the same signed angular delta on both access paths: direct BLE applies it at the node, while the bridge sends the resulting two-axis value as an idempotent absolute-target transaction. Stop retains identical halt semantics. Both operations were exercised on the assembled system.

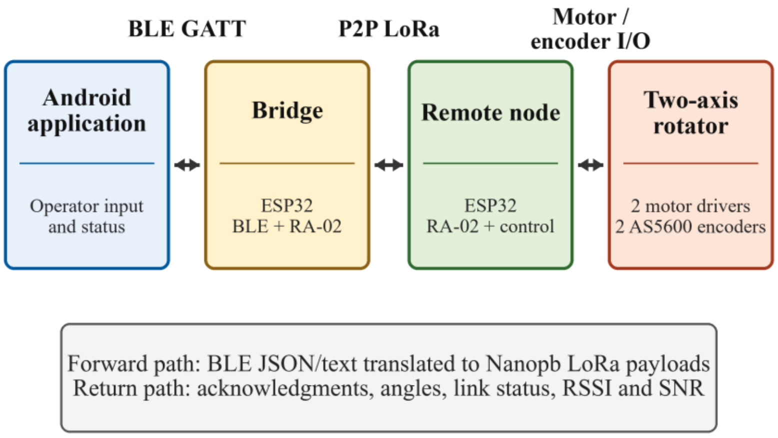

Figure 1
Command and feedback paths of the implemented ESP32 BLE-to-LoRa antenna-pointing system
Source: Prepared by the authors.

The assembled bridge unit used in the hardware-in-the-loop campaign is shown in Fig. 2. The closed enclosure provides a compact operator-side device, while the internal view documents the installed ESP32 controller, rechargeable cell, power switch, antenna, and interconnection board.

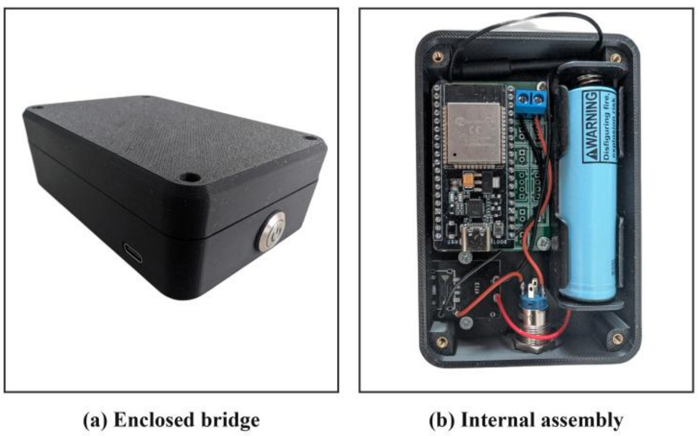

Figure 2
Implemented BLE-to-LoRa bridge: (a) closed enclosure; (b) internal assembly
Source: Authors' photographic archive.

Materials and methods. The hardware-in-the-loop evaluation used the assembled two-axis rotator, two ESP32 and RA-02 nodes, the bridge shown in Fig. 2, and Android terminals. Six successive iterations exercised direct BLE, relayed BLE-to-LoRa, and Internet access. The 43-item plan covered access, configuration, manual and automatic control, transport parity, recovery, and user-interface functions. A full pass required the commanded function, returned state, and safety response to meet the stated acceptance condition; partial and failed outcomes were recorded separately. Six items requiring destructive intervention, an unavailable simultaneous-access rig, or a human-only gesture were explicit exclusions from the executed-item denominator. Table 1 summarizes the hardware and protocol configuration.

Table 1

Hardware and protocol configuration

Subsystem	Implementation	Parameter	Value
Local access	ESP32 BLE GATT	BLE MTU	247 bytes
Secure LoRa frame	AES-256-GCM	Header / IV / tag / payload	19 / 12 / 16 / ≤200 bytes
Bridge radio	ESP32 + RA-02	Carrier / BW / SF / CR / power	433.0 MHz / 125 kHz / 7 / 4/5 / 14 dBm
Reliable flows	Precise target and stop	ACK timeout per transmitted attempt / maximum retries	1500 ms / 2
Remote node	ESP32 + RA-02	LoRa full telemetry	4000 ms
Rotator	2 × BTS7960 + 2 × AS5600	Manual / auto and parking tolerance	0.35 / 1.5 degrees

Source: Maintained firmware configuration and assembled hardware.

LoRa application messages used Advanced Encryption Standard 256-bit Galois/Counter Mode (AES-256-GCM). A secure frame contains a 19-byte header, 12-byte initialization vector, 16-byte authentication tag, and at most 200 plaintext bytes, for a maximum serialized size of 247 bytes. Reliable precise-target and stop transactions wait 1500 ms after confirmed transmission and permit two retries. The half-duplex scheduler uses a 60 ms cooldown, 500 ms listen-after-talk interval, randomized 20–79 ms busy-channel backoff, and a six-item first-in, first-out queue.

Formula (1) defines the descriptive full-pass rate for the executed test set. The denominator includes full passes, partial results, and failures; explicitly excluded items remain visible in Table 2 but are not treated as executed or passed. This measure describes the proportion of fully passed items among the executed system tests and is not a probability-of-failure estimate.

$$R_{pass} = \frac{N_{pass}}{N_{exec}} \times 100\%, \qquad (1)$$

where R_{pass} – descriptive full-pass rate for executed system tests, percent; N_{pass} – executed test items meeting every acceptance criterion; N_{exec} – all executed items, including partial results and failures.

Formula (2) gives the maximum settled two-axis pointing error. For completed coordinate-pointing cases, the endpoint values were read from node telemetry after the controller reported target lock. The same metric was applied to direct and relayed observations, and the result was compared with the implemented 1.5-degree automatic-control tolerance.

$$e_{max} = \max_{k \in \{az,el\}} \left| \theta_{target,k} - \theta_{measured,k} \right| \qquad (2)$$

where e_{max} – maximum settled two-axis error, degrees; k – axis index: azimuth or elevation; $\theta_{target,k}$ – commanded angle for axis k, degrees; $\theta_{measured,k}$ – settled encoder reading for axis k, degrees.

Experimental results and discussion. The completed campaign produced 34 full passes, one partial result, and two failures among 37 executed items; six plan items were explicitly excluded. Formula (1) therefore gives a descriptive full-pass rate of 91.9%. Table 2 shows that all 20 access, configuration, and manual-control items passed, while both full failures were concentrated in mutual peer-session operation rather than general bridge transport or pointing control.

Table 2

Completed hardware-in-the-loop test matrix

Functional group	Planned	Full pass	Partial	Fail	Excluded
Access and connection	5	5	0	0	0
Configuration and provisioning	8	8	0	0	0
Manual control	7	7	0	0	0
Automatic control	7	4	0	2	1
Transport parity	5	3	1	0	1
Failure recovery	7	4	0	0	3
User interface	4	3	0	0	1
Total	43	34	1	2	6

Source: Completed hardware-in-the-loop test records.

The direct and relayed precise-jog tests reproduced signed 5-degree increments on both axes. Coordinate pointing produced a maximum observed settled two-axis error of approximately 1.3 degrees over direct BLE and 1.0 degree over the bridge; both values were within the 1.5-degree automatic-control tolerance. During the bridge-specific 30 s manual hold, all 126 recorded samples reported an authenticated, linked state, with received signal strength indicator (RSSI) from −79 to −77 dBm and signal-to-noise ratio (SNR) from 9.2 to 12.0 dB. Direct and bridge access also recovered cleanly after an induced Bluetooth interruption. Table 3 summarizes the principal quantitative observations.

Table 3

Principal hardware-in-the-loop observations

Observation	Direct BLE	BLE-to-LoRa bridge	Assessment
Signed precise jog	±5 degrees reproduced on both axes	±5 degrees reproduced on both axes	Command sign and increment confirmed
Maximum settled two-axis error	Approx. 1.3 degrees	Approx. 1.0 degree	Both within the 1.5-degree tolerance
30 s bridge hold	Reference path not required	126 of 126 samples reported link up	Stable relayed status during the observation

Table continuation 3

Mutual peer session	Established with common session state	0 of 2 relay attempts established	Reproducible failure isolated for diagnosis
Access interruption and recovery	Clean reconnection	Clean reconnection and telemetry return	Recovery behavior passed

Source: Completed hardware-in-the-loop observations.

The two full failures were a bridge-mediated mutual session and a cross-transport mutual-session observation. A serial-instrumented diagnostic iteration then established a mutual session without bridge traffic in approximately 1.5 s and captured its collapse after approximately 78 s through five recurring peer-stale cycles. Both nodes lost two to four consecutive peer-telemetry frames while RSSI remained between −68 and −54 dBm and SNR between 9.2 and 10.8 dB. Neither node recorded an application-layer discard, and the idle node exhibited the same loss pattern without local operator ingress. Table 4 presents the resulting causal chain and corrective action.

Table 4

Failure-mechanism evidence and corrective action

Evidence step	Observation	Technical interpretation
Session timeline	Handshake converged in approx. 1.5 s; a diagnostic session ended after approx. 78 s through five peer-stale cycles	Failure could occur without active bridge or operator traffic
Radio reception	Two to four consecutive peer frames were absent on both nodes while RSSI was −68 to −54 dBm and SNR was 9.2 to 10.8 dB	Weak received signal was not the primary cause
Application processing	No application-layer discard was recorded; the idle node showed the same pattern	Loss occurred before command-ingress handling
Transmit-path audit	The immediate LoRa transmit branch bypassed clear-channel assessment used by the queued branch	One mechanism explained direct-peer and bridge-triggered contention
Corrective action	Channel-busy assessment was added to the immediate guard; busy frames enter the existing queue and randomized backoff	The maintained firmware now applies consistent half-duplex arbitration

Source: Retained serial captures and firmware transmit-path analysis.

The combined evidence excludes weak received signal, BLE command ingress, and application-layer rejection as the primary mechanism. The transmit-path audit identified a consistency defect: immediate LoRa transmissions could begin without clear-channel assessment, whereas queued transmissions assessed the channel and applied randomized backoff. The corrective guard routes a busy immediate transmission into the existing queue, preserving priority and retry behavior. The corrected firmware passed both production-node and bench-simulation builds and was incorporated into the maintained implementation. Because the direct and relayed error observations came from separate operating portions, their 0.3-degree difference is descriptive rather than evidence of statistical superiority; the supported result is that both remained within the implemented tolerance.

Funding disclosure. This study received no external funding.

Data availability. The consolidated test matrix and retained serial captures supporting the diagnostic findings are preserved in the project archive and are available from the corresponding author on reasonable request.

Conclusions. An ESP32 and RA-02 bridge was assembled, integrated into a two-axis antenna rotator, and evaluated in a completed hardware-in-the-loop campaign. Of 37 executed system tests, 34 met every acceptance criterion, giving a descriptive full-pass rate of 91.9%; one result was partial and two reproducible failures affected the same mutual peer-session function. Direct and relayed 5-degree jogs executed correctly, coordinate-pointing error remained within the 1.5-degree control tolerance, and all 126 bridge-hold samples reported the link up. Retained serial evidence localized the mutual-session failures to an immediate LoRa transmission branch that bypassed clear-channel assessment despite healthy RSSI and SNR. Integrating the same channel-busy guard used by the queued path closed this scheduling inconsistency while preserving the existing priority and backoff mechanism. The scientific contribution is a hardware-validated BLE-to-LoRa control architecture and an experimentally grounded requirement that every half-duplex transmit branch apply consistent channel arbitration.

References:

[1] Hamajima, K., Yasukawa, K., Ueba, M., Kanou, H., Matsui, M., Abe, J., Itokawa, K., & Yamashita, F. (2023). Design and evaluation on onboard antenna pointing control system for a wireless relay system using fixed-wing UAV. Aerospace, 10(4), 323. https://doi.org/10.3390/aerospace10040323

[2] Fakhri, M., Rahmat, M. Z., Pascawati, A., Harsono, S. D., Nugroho, Y. W., Rahardiyanti, K., & Rohmah, N. F. (2024). Dual-mode antenna tracking system for rocket launch applications. Jurnal Rekayasa Elektrika, 20(2), 49-57. https://doi.org/10.17529/jre.v20i2.35043

[3] Sarmento, T., Nakamura, A., Filho, I., Correa, L., Takeda, M., Castro, A., & Klautau, A. (2018). Development and evaluation of least square satellite tracking in real antenna control system. Proceedings of the XXXVI Brazilian Telecommunications and Signal Processing Symposium. https://doi.org/10.14209/sbrt.2018.142

[4] Guo, Q., Yang, F., & Wei, J. (2021). Experimental evaluation of the packet reception performance of LoRa. Sensors, 21(4), 1071. https://doi.org/10.3390/s21041071

[5] Cattani, M., Boano, C. A., & Römer, K. (2017). An experimental evaluation of the reliability of LoRa long-range low-power wireless communication. Journal of Sensor and Actuator Networks, 6(2), 7. https://doi.org/10.3390/jsan6020007

[6] Liang, R., Zhao, L., & Wang, P. (2020). Performance evaluations of LoRa wireless communication in building environments. Sensors, 20(14), 3828. https://doi.org/10.3390/s20143828

[7] Guerrero, M., Cano, C., Vilajosana, X., & Thubert, P. (2021). Towards dependable IoT via interface selection: Predicting packet delivery at the end node in LoRaWAN networks. Sensors, 21(8), 2707. https://doi.org/10.3390/s21082707

[8] Tamang, D., Pozzebon, A., Parri, L., Fort, A., & Abrardo, A. (2022). Designing a reliable and low-latency LoRaWAN solution for environmental monitoring in factories at major accident risk. Sensors, 22(6), 2372. https://doi.org/10.3390/s22062372

[9] Montgomery, K., Kashef, M., & Candell, R. (2024). Latency-sensitive networked control using 802.11ax OFDMA triggering. Proceedings of the 2024 IEEE/ASME International Conference on Advanced Intelligent Mechatronics, 1088-1095. https://doi.org/10.1109/AIM55361.2024.10637136

[10] Semtech Corporation. (2020). SX1276/77/78/79 wireless and sensing products datasheet, revision 7. https://www.semtech.com/products/wireless-rf/lora-connect/sx1276

[11] Espressif Systems. (2026). ESP32 series datasheet, version 5.3. https://documentation.espressif.com/esp32_datasheet_en.pdf

[12] Bluetooth Special Interest Group. (2024). Core specification (amended) 4.2 (core package published 2 December 2014; amended 11 June 2024). https://www.bluetooth.com/specifications/specs/core-specification-amended-4-2/